Journal of Geophysical Research Biogeosciences

Supporting Information for

Optimizing Phenology Parameters Drastically Improves Terrestrial Biosphere Model Underestimates of Dryland Net CO_2 Flux Inter-Annual Variability

Kashif Mahmud[1], Russell L. Scott[2], Joel A. Biederman[2], Marcy E. Litvak[3], Thomas Kolb[4], Tilden P. Meyers[5], Praveena Krishnan[5,6], Vladislav Bastrikov[7,8], and Natasha MacBean[1]

[1]Department of Geography, Indiana University, Bloomington, IN 47405, USA

[2]Southwest Watershed Research Center, United States Department of Agriculture, Agricultural Research Service, Tucson, AZ 85719, USA

[3]Department of Biology, University of New Mexico, Albuquerque, NM, 87131, USA

[4]School of Forestry, Northern Arizona University, Flagstaff, AZ, 86011, USA

[5]NOAA/ARL Atmospheric Turbulence and Diffusion Division, Oak Ridge, TN, 37830, USA

[6]Oak Ridge Associated Universities, Oak Ridge, TN, 37830, USA

[7]Laboratoire des Sciences du Climat et de l'Environnement, LSCE/IPSL, CEA-CNRS-UVSQ, Université Paris-Saclay, Gif-sur-Yvette, F-91191, France

[8]Now at: Science Partners, Paris, 75010, France

Contents of this file

Table S1. Prior information for all ORCHIDEE parameters optimized in this study: prior value, uncertainty and maximum and minimum bounds for the different plant functional types (temperate needleleaf/broadleaf evergreen (TeNE, TeBE) forests, temperate broadleaf deciduous (TeBD) forest, C4 grassland (GC4)).

Parameter Name	Description (Unit)	Plant functional type			
		TeNE	TeBE	TeBD	GC4
Photosynthesis parameters					
ARJV	a coefficient of the linear regression (a+bT) defining the Jmax25/Vcmax25 ratio (mu mol e- (mu mol CO_2)-1)	2.59 ± 0.4 2, 3	2.59 ± 0.4 2, 3	2.59 ± 0.4 2, 3	1.715 ± 0.48 1, 2.2
aSJ	a coefficient of the linear regression (a+bT) defining the Entropy term for Jmax (J K-1 mol-1)	659.7 ± 264 330, 990	659.7 ± 264 330, 990	659.7 ± 264 330, 990	630 ± 252 315, 945
aSV	a coefficient of the linear regression (a+bT) defining the Entropy term for Vcmax (J K-1 mol-1)	668.39 ± 267.6 334, 1003	668.39 ± 267.6 334, 1003	668.39 ± 267.6 334, 1003	641.64 ± 256.4 321, 962
BRJV	b coefficient of the linear regression (a+bT) defining the Jmax25/Vcmax25 ratio (mu mol e- (mu mol CO_2)-1)	-0.035 ± 0.028 -0.07, 0	-0.035 ± 0.028 -0.07, 0	-0.035 ± 0.028 -0.07, 0	-0.01 ± 0.028 -0.035, 0.035
bSJ	b coefficient of the linear regression (a+bT) defining the Entropy term for Jmax (J K-1 mol-1 C-1)	-0.75 ± 0.6 -1.5, 0	-0.75 ± 0.6 -1.5, 0	-0.75 ± 0.6 -1.5, 0	0.01 ± 0.6 -0.75, 0.75
bSV	b coefficient of the linear regression (a+bT) defining the Entropy term for Vcmax (J K-1 mol-1 C-1)	-1.07 ± 0.8 -2, 0	-1.07 ± 0.8 -2, 0	-1.07 ± 0.8 -2, 0	0.1 ± 0.856 -1.07, 1.07
CN	C/N ratio	40 ± 32 20, 100	40 ± 32 20, 100	40 ± 32 20, 100	-
D_Jmax	Energy of deactivation for Jmax (J/mol)	200000 ± 16000 180000, 220000	200000 ± 16000 180000, 220000	200000 ± 16000 180000, 220000	192000 ± 15200 173000, 211000
D_Vcmax	Energy of deactivation for Vcmax (J/mol)	200000 ± 16000 180000, 220000	200000 ± 16000 180000, 220000	200000 ± 16000 180000, 220000	192000 ± 15200 173000, 211000
E_gamma_star	Energy of activation for gamma_star (J mol-1)	37830 ± 8000 27830, 47830	37830 ± 8000 27830, 47830	37830 ± 8000 27830, 47830	37830 ± 8000 27830, 47830
E_Jmax	Energy of activation for Jmax (J mol-1)	49884 ± 8000 39884, 59884	49884 ± 8000 39884, 59884	49884 ± 8000 39884, 59884	77900 ± 8000 67900, 87900
E_KmC	Energy of activation for KmC (J mol-1)	79430 ± 8000 69430, 89430	79430 ± 8000 69430, 89430	79430 ± 8000 69430, 89430	79430 ± 8000 69430, 89430
E_KmO	Energy of activation for KmO (J mol-1)	36380 ± 8000 26380, 46380	36380 ± 8000 26380, 46380	36380 ± 8000 26380, 46380	36380 ± 8000 26380, 46380
fpseudo	Fraction of electrons at PSI that follow pseudocyclic transport	-	-	-	0.1 ± 0.032 0.06, 0.14
fpsir	Fraction of PSII e−transport rate partitioned to the C4 cycle	-	-	-	0.4 ± 0.16 0.4, 0.6
FRAC_GROWTHRESP	Fraction of GPP which is lost as growth respiration	0.28 ± 0.064 0.2, 0.36	0.28 ± 0.064 0.2, 0.36	0.28 ± 0.064 0.2, 0.36	0.28 ± 0.064 0.2, 0.36

fQ	Fraction of electrons at reduced plastoquinone that follow the Q-cycle	-	-	-	1 ± 0.24 0.7, 1.3
gamma_star25	Ci-based CO_2 compensation point in the absence of Rd at 25C (ubar)	42.75 ± 8 22.75, 62.75	42.75 ± 8 22.75, 62.75	42.75 ± 8 22.75, 62.75	42.75 ± 8 22.75, 62.75
gbs	Bundle-sheath conductance (mol m-2 s-1 bar-1)	-	-	-	0.003 ± 0.0008 0.001, 0.005
HYDROL_HUMCSTE	Root profile (m) in empirical plant water stress function calculation	1 ± 1.5 0.25, 4	0.8 ± 1.12 0.2, 3	0.8 ± 1.12 0.2, 3	1 ± 1.5 0.25, 4
KmC25	Michaelis-Menten constant of Rubisco for CO_2 at 25C (ubar)	404.9 ± 160 204.9, 604.9	404.9 ± 160 204.9, 604.9	404.9 ± 160 204.9, 604.9	650 ± 160 450, 850
KmO25	Michaelis-Menten constant of Rubisco for O_2 at 25C (ubar)	278400 ± 80000 178400, 378400	278400 ± 80000 178400, 378400	278400 ± 80000 178400, 378400	450000 ± 80000 350000, 550000
kp	Initial carboxylation efficiency of the PEP carboxylase (mol m-2 s-1 bar-1)	-	-	-	0.7 ± 0.24 0.4, 1
LAI_MAX	Maximum LAI (m2/m2)	5 ± 2 3, 8	5 ± 2 3, 8	5 ± 2 3, 8	2.5 ± 0.8 4, 10
Sco25	Relative CO_2 /O_2 specificity factor for Rubisco at 25C (bar bar^{-1})	2800 ± 800 1800, 3800	2800 ± 800 1800, 3800	2800 ± 800 1800, 3800	2590 ± 800 1590, 3590
SLA	Specific leaf area (m2/gC)	0.00926 ± 0.005 0.004, 0.02	0.02 ± 0.012 0.01, 0.04	0.026 ± 0.0148 0.013, 0.05	0.026 ± 0.0148 0.013, 0.05
theta	Convexity factor for response of J to irradiance	0.7 ± 0.18 0.5, 0.95	0.7 ± 0.18 0.5, 0.95	0.7 ± 0.18 0.5, 0.95	0.7 ± 0.18 0.5, 0.95
TPHOTO_MAX	Maximum photosynthesis temperature (deg C)	55 ± 4 50, 60	55 ± 4 50, 60	55 ± 4 50, 60	55 ± 4 50, 60
TPHOTO_MIN	Minimum photosynthesis temperature (deg C)	-4 ± 4 -9, 1	-4 ± 4 -9, 1	-4 ± 4 -9, 1	-4 ± 4 -9, 1
VCMAX25	Maximum rate of Rubisco activity-limited carboxylation at 25C (micromol/m2/s)	35 ± 10 19, 51	45 ± 16 25, 65	55 ± 20 30, 80	70 ± 25.6 38, 102
VMAX_OFFSET	Offset (minimum relative vcmax)	0.3 ± 0.048 0.24, 36			
Post C uptake parameters - autotrophic and heterotrophic respiration, C allocation, biomass and soil C turnover					
HCRIT_LITTER	Scaling depth for litter humidity (m)	0.08 ± 0.192 0.02, 0.5			
KSOILC	Scalar on the active soil C pool content (to account for uncertainty in spin-up)	1 ± 0.6 0.5, 2			
MAINT_RESP_COEFF	Coefficient to calculate maintenance respiration as a fraction of biomass	1.4 ± 0.84 0.7, 2.4			
MAINT_RESP_SLOPE_C	Slope of maintenance respiration coefficient (1/K), constant c of aT^2+bT+c, tabulated	0.16 ± 0.064 0.08, 0.24	0.16 ± 0.064 0.08, 0.24	0.16 ± 0.064 0.08, 0.24	0.12 ± 0.06 0.04, 0.2
MAX_LTOLSR	Extrema of leaf allocation fraction	0.5 ± 0.08 0.4, 0.6			
MIN_LTOLSR	Extrema of leaf allocation fraction	0.2 ± 0.08 0.1, 0.3			
MOIST_COEFF__1	Coefficient to calculate moisture control for litter and soil C decomposition	1.1 ± 0.24 0.8, 1.4			
MOIST_COEFF__2	Coefficient to calculate moisture control for litter and soil C decomposition	2.4 ± 0.24 2.1, 2.7			
MOIST_COEFF__3	Coefficient to calculate moisture control for litter and soil C decomposition	0.29 ± 0.232 0.01, 0.59			
MOISTCONT_MIN	Minimum soil wetness to limit the heterotrophic respiration	0.25 ± 0.2 0.1, 0.6			

RESIDENCE_TIME	Residence time of trees (years)	40 ± 24 30, 90	40 ± 24 30, 90	40 ± 24 30, 90	0 ± 0 0,0
SOIL_Q10	Temperature dependency factor for heterotrophic respiration (Note: actual Q10 = exp^{SOIL_Q10}.	0.69 ± 0.44 0, 1.1			
TAU_FRUIT	Fruit lifetime (days)	90 ± 24 60, 120	90 ± 24 60, 120	90 ± 24 60, 120	-
TAU_METABOLIC	A coefficient to calculate residence times in metabolic litter pools (days)	0.066 ± 0.0112 0.052, 0.08			
TAU_SAP	Sapwood heartwood conversion time (days)	730 ± 144 550, 910	730 ± 144 550, 910	730 ± 144 550, 910	-
TAU_STRUCT	A coefficient to calculate residence times in structural litter pools (days)	0.245 ± 0.04 0.2, 0.3			
Phenology parameters					
GDD_THRESHOLD	Temperature threshold used in the calculation of number of growing degree day, GDD (days)	5 ± 0.8 4, 6			
GDDNCD_CURVE	Constant in the computation of critical GDD	0.0091 ± 0.00112 0.0072, 0.01			
GDDNCD_OFFSET	Constant in the computation of critical GDD (days)	64 ± 11.2 50, 78			
GDDNCD_REF	Reference value used in the computation of critical GDD (days)	603 ± 96.8 482, 724			
HUM_FRAC	Critical humidity (relative to min/max) for phenology (%)	-	-	-	0.5 ± 0.2 0.25, 0.75
HUM_MIN_TIME	Minimum time elapsed since moisture minimum (days)	-	-	-	35 ± 12 20, 50
LAI_MAX_TO_HAPPY	Threshold of LAI below which plant uses carbohydrate reserves	0.5 ± 0.14 0.35, 0.7	0.5 ± 0.14 0.35, 0.7	0.5 ± 0.14 0.35, 0.7	0.5 ± 0.14 0.35, 0.7
LEAF_AGE_CRIT_COEF_1	A coefficient to calculate critical leaf age (days)	1.5 ± 0.24 1.2, 1.8			
LEAF_AGE_CRIT_COEF_2	A coefficient to calculate critical leaf age (days)	0.75 ± 0.12 0.6, 0.9			
LEAF_AGE_CRIT_COEF_3	A coefficient to calculate critical leaf age (days)	10 ± 1.6 12, 8			
LEAF_AGE_CRIT_TREF	Reference temperature used to calculate of critical leaf age (days)	20 ± 4 15, 25			
LEAFAGE_FIRSTMAX	Leaf age at which vmax attains vcmax_opt (in fraction of critical leaf age)	0.03 ± 0.0048 0.024, 0.036			
LEAFAGE_LASTMAX	Leaf age at which vmax falls below vcmax_opt (in fraction of critical leaf age)	0.5 ± 0.08 0.4, 0.6			
LEAFAGECRIT	Critical leaf age, tabulated (days)	910 ± 200 610, 1210	730 ± 192 490, 970	180 ± 60 120, 240	120 ± 60 30, 180
LEAFFALL	Length of death of leaves, tabulated (days)	-	-	10 ± 4 5, 15	10 ± 4 5, 15
LEAFLIFE_TAB	Leaf longevity (years)	0.33 ± 0.1 0.2, 0.75	1 ± 0.668 0.33, 2	2 ± 0.9 0.75, 3	2 ± 0.9 0.75, 3
MAX_TURNOVER_TIME	Maximum turnover time for grass (days)	-	-	-	80 ± 4 75, 85
MIN_GROWTHINIT_TIME	Minimum time since last beginning of a growing season (days)	300 ± 24 270, 330			
MIN_LEAF_AGE_FOR_SENESCENCE	minimum leaf age to allow senescence (days)	-	-	90 ± 8 80, 100	30 ± 4 25, 35
MIN_TURNOVER_TIME	Minimum turnover time for grass (days)	-	-	-	10 ± 4 5, 15

NCD_MAX_YEAR	A coefficient to calculate maximum possible number of chilling days (NCD)	3 ± 0.8 2, 4			
NCDGDD_TEMP	Critical temperature for the ncd vs. gdd function in phenology (C)	-	-	5 ± 4 0, 10	-
NOSENESCENCE_HUM	Relative moisture availability above which there is no humidity-related senescence	-	-	-	0.3 ± 0.12 0.15, 0.45
PHENO_GDD_CRIT_A	Critical gdd tabulated constant a	-	-	-	0 ± 0 0, 0
PHENO_GDD_CRIT_B	Critical gdd constant b	-	-	-	0 ± 0 0, 0
PHENO_GDD_CRIT_C	Critical gdd constant c	-	-	-	400 ± 64 320, 480
PHENO_MOIGDD_T_CRIT	Average temperature threshold for C4 grass used (C)	-	-	-	22 ± 8 12, 32
SENESCENCE_HUM	Critical relative moisture availability for senescence	-	-	-	0.2 ± 0.08 0.1, 0.3
SENESCENCE_TEMP_A	Critical temperature for senescence (C), constant a of aT^2+bT+c, tabulated	-	-	0 ± 0 0, 0	0 ± 0 0, 0
SENESCENCE_TEMP_B	Critical temperature for senescence (C), constant b of aT^2+bT+c, tabulated	-	-	0 ± 0 0, 0	0 ± 0 0, 0
SENESCENCE_TEMP_C	Critical temperature for senescence (C), constant c of aT^2+bT+c, tabulated	-	-	12 ± 8 2, 22	5 ± 4.8 -1, 11
TAU_CLIMATOLOGY	tau for climatologic variables (days)	20 ± 8 10, 30			
TAU_GDD	Time scales for phenology and other processes (days)	40 ± 16 20, 60			
TAU_GPP_WEEK	Time scales for phenology and other processes (days)	6 ± 1 5, 7			
TAU_HUM_MONTH	Time scales for phenology and other processes (days)	20 ± 8 10, 30			
TAU_HUM_WEEK	Time scales for phenology and other processes (days)	6 ± 1 5, 7			
TAU_LEAFINIT	Time to attain the initial foliage using the carbohydrate reserve (days)	10 ± 10 5, 30	10 ± 10 5, 30	10 ± 10 5, 30	10 ± 10 5, 30
TAU_NGD	Time scales for phenology and other processes (days)	50 ± 20 25, 75			
TAU_SOILHUM_MONTH	Time scales for phenology and other processes (days)	20 ± 8 10, 30			
TAU_T2M_MONTH	Time constant for the “monthly” 2-meter temperature (days)	20 ± 8 10, 30			
TAU_T2M_WEEK	Time constant for the “weekly” 2-meter temperature (days)	6 ± 1 5, 7			
TAU_TSOIL_MONTH	Time constant for the “monthly” soil temperature (days)	20 ± 8 10, 30			
Conductance parameters - included in initial optimization sensitivity test but not in final optimizations					
A1	empirical factor involved in the calculation of fvpd	0.85 ± 0.04 0.8, 0.9	0.85 ± 0.04 0.8, 0.9	0.85 ± 0.04 0.8, 0.9	0.85 ± 0.04 0.8, 0.9
B1	empirical factor involved in the calculation of fvpd	0.14 ± 0.032 0.1, 0.18	0.14 ± 0.032 0.1, 0.18	0.14 ± 0.032 0.1, 0.18	0.2 ± 0.032 0.15, 0.25
CHOISNEL_RSOL_CSTE	Constant in the computation of resistance for bare soil evaporation (s/m2)	3.3E4 ± 19400 1.75E4, 6.6E4			
CONDVEG_Z0	Surface roughness (m)	0.15 ± 0.12 0, 0.3			
DEFC_MULT	Constant in the computation of surface resistance (KW^{-1})	1.5 ± 0.9 0.75, 3			
DEFC_PLUS	Constant in the computation of surface resistance (KW^{-1})	0.023 ± 0.016 0.003, 0.043			

g0	Residual stomatal conductance when irradiance approaches zero (mol m-2 s-1 bar-1)	0.00625 ± 0.00048 0.00565, 0.00685	0.00625 ± 0.00048 0.00565, 0.00685	0.00625 ± 0.00048 0.00565, 0.00685	0.01875 ± 0.0016 0.01675, 0.02075
GB_REF	Leaf bulk boundary layer resistance (s m-1)	0.04 ± 0.032 0, 0.08			
KZERO	A vegetation dependent constant used in the calculation of the surface resistance (kg/m^2/s)	0.00012 ± 0.000016 0.0001, 0.00014	0.00012 ± 0.000016 0.0001, 0.00014	0.00025 ± 0.00004 0.0002, 0.0003	0.0003 ± 0.00004 0.00025, 0.00035
RATIO_Z0M _Z0H	Ratio between z0m and z0h	1 ± 0.4 0.5, 1.5	1 ± 0.4 0.5, 1.5	1 ± 0.4 0.5, 1.5	1 ± 0.4 0.5, 1.5
Z_DECOMP	Scaling depth for soil activity	0.2 ± 0.6 0, 1.5			
Z0_BARE	Bare soil roughness length (m)	0.01 ± 0.0016 0.008, 0.012			
Z0_OVER_H EIGHT	To get z0 from height	0.0625 ± 0.032 0.02, 0.1			

Table S2. Daily GPP and ecosystem respiration (R_{eco}) model-data fit when assimilating NEE observations with all parameters (P1) in terms of prior and posterior root mean square error (RMSE) for all twelve sites. The reduction in daily GPP RMSE varies between 0 to 0.55 $gCm^{-2}d^{-1}$, and the reduction in daily R_{eco} RMSE varies between 0 to 0.5 $gCm^{-2}d^{-1}$. The sites are listed in order from largest mean annual C sink (US-Vcm) to mean annual C source (US-Aud).

Site	Daily root mean square error (RMSE)			
	GPP		R_{eco}	
	Prior	Posterior	Prior	Posterior
US-Vcm	1.402	1.473	1.967	1.433
US-Vcp	1.803	1.26	0.941	1.019
US-Mpj	1.294	0.917	0.943	0.804
US-Fuf	0.989	0.789	0.532	0.655
US-Wjs	1.046	0.77	0.766	0.699
US-Ses	0.272	0.308	0.238	0.313
US-Wkg	1.08	0.524	0.577	0.386
US-SRG	1.298	0.887	0.93	0.756
US-Seg	0.689	0.485	0.429	0.354
US-SRM	1.167	0.64	0.811	0.578
US-Whs	0.65	0.547	0.477	0.445
US-Aud	1.092	0.817	0.51	0.604

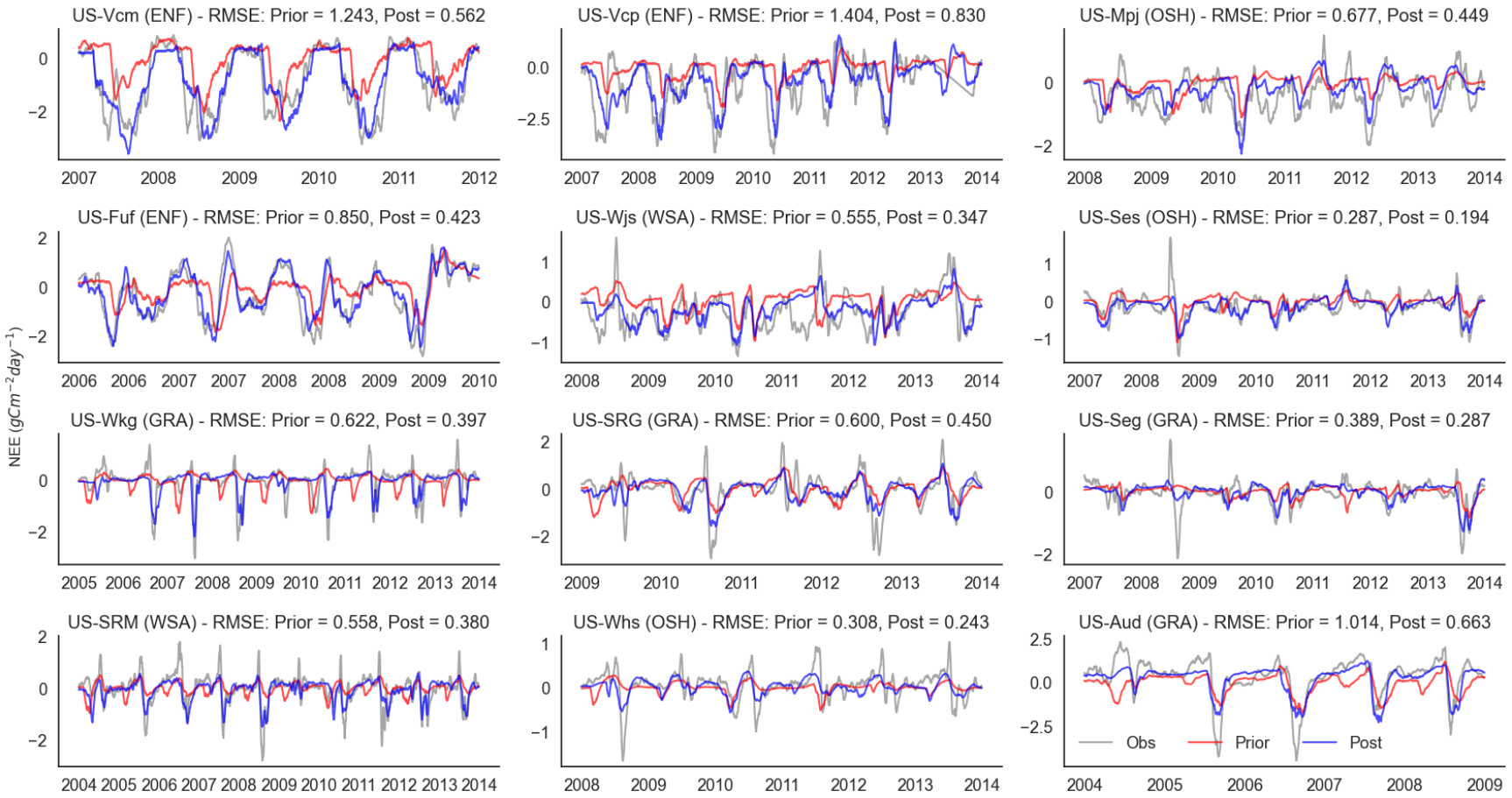

Figure S1. Comparison of NEE observations (grey) with corresponding ORCHIDEE model simulations before (red line) and after assimilation (blue line) for assimilating NEE observations with all parameters (P1). The vegetation types are listed within brackets for each site. The RMSE measures the fit of the model prior and posterior simulations with the corresponding observations. Across all sites, the prior and posterior NEE RMSEs vary between 0.291-1.377 and 0.196-0.788, respectively. The sites are listed in order from largest mean annual C sink (US-Vcm) to mean annual C source (US-Aud).

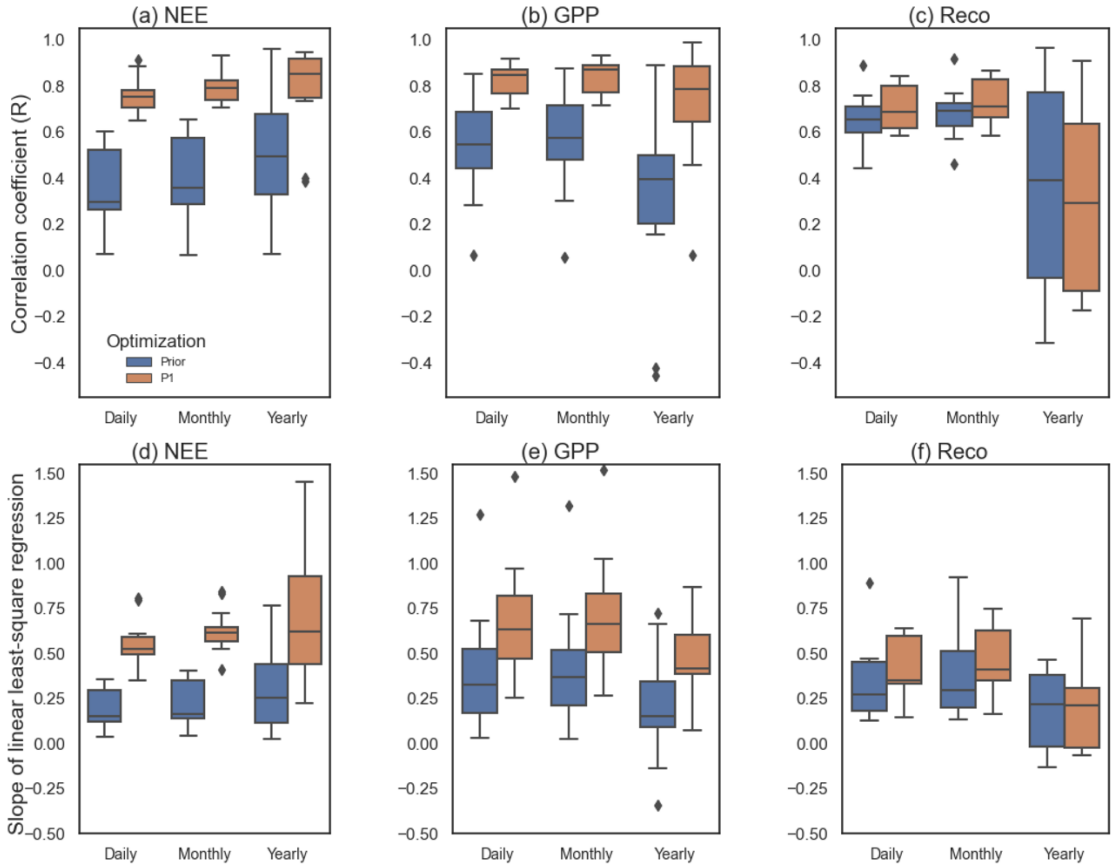

Figure S2. Daily, monthly and annual NEE (a, d), GPP (b, e) and R_{eco} (c, f) prior and posterior Pearson correlation coefficients (R) and slope values for the linear regression between model and observed fluxes for assimilating NEE observations and optimizing all phenology, photosynthesis and post C uptake parameters (P1). The R between observed and modeled NEE at daily, monthly and annual timescales for optimizing all parameters (P1) increase by up to 0.50, 0.55, 0.65 respectively. Note that the y axis limits for both R and slope are the same and therefore 3 sites fall outside the y-axis upper limit for the R_{eco} slope.

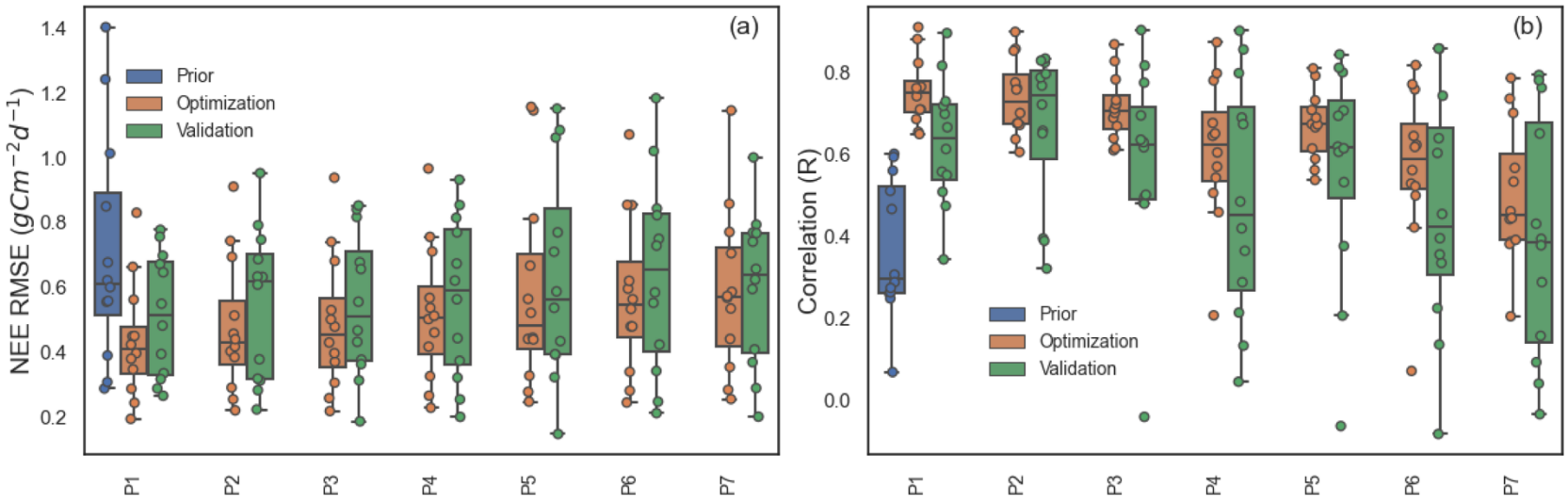

Figure S3. Comparison between the posterior RMSE and R for both optimization (orange bars) and validation (green bars) simulations of daily NEE. The prior RMSE and R values are also shown in blue bars. The last year of NEE time series for each site is used for the validation purpose. The box-whiskers indicate the spread of RMSE and R ratios for all 12 sites.

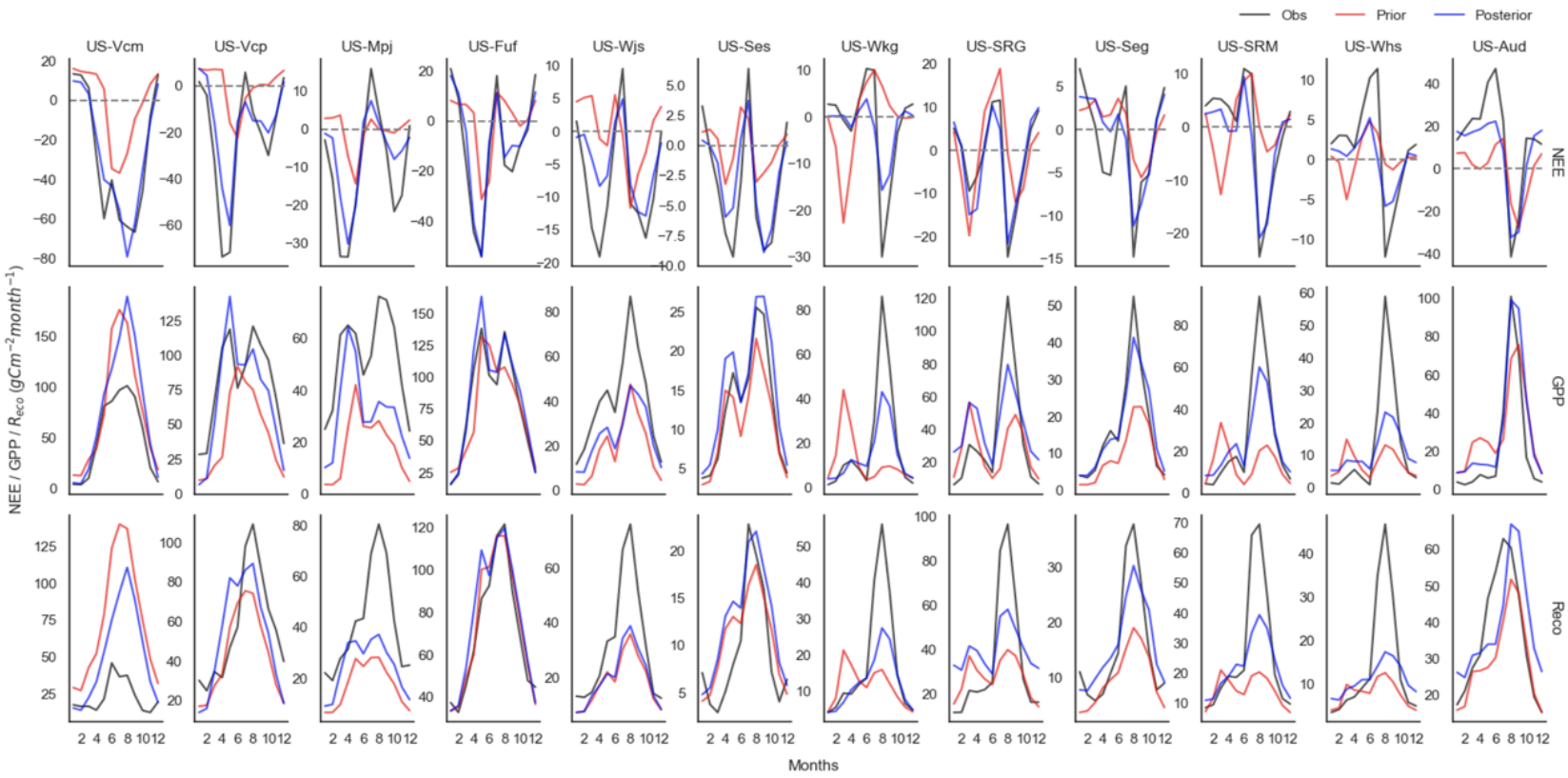

Figure S4. Seasonal cycle with mean monthly total fluxes. Comparison of flux observations with corresponding ORCHIDEE model simulations (prior and posterior) for assimilating NEE observations and optimizing all phenology, photosynthesis and post C uptake parameters (P1). The sites are listed from left to right according to C sink to source.

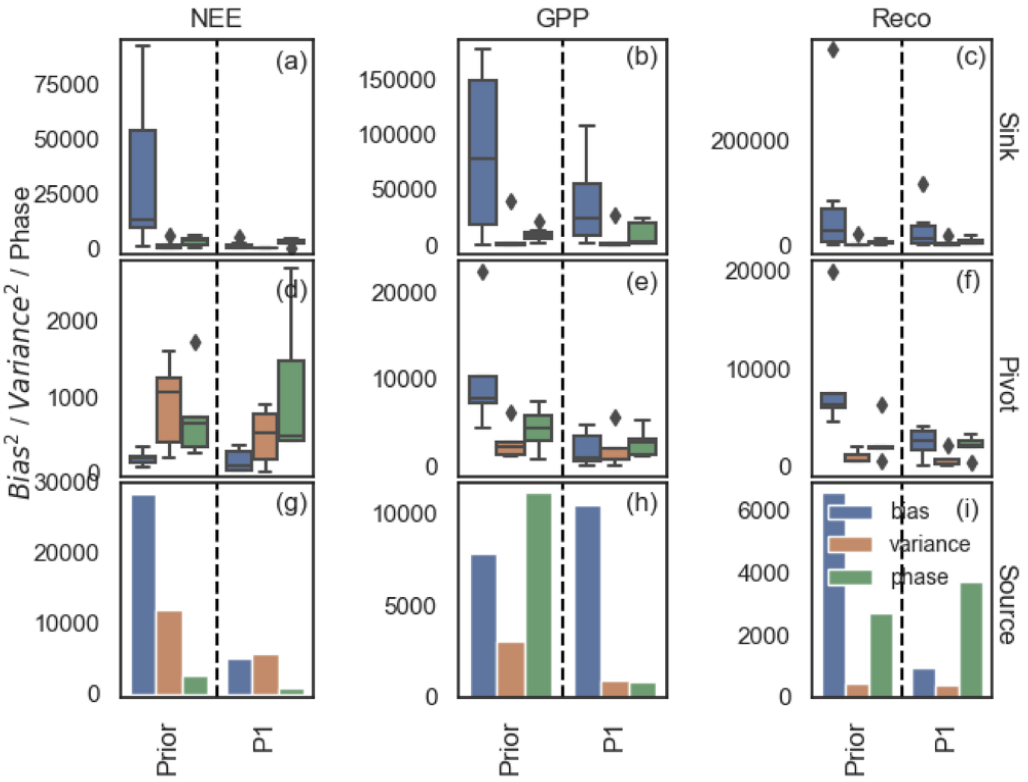

Figure S5. Annual NEE, GPP and R_{eco} mean square deviation (MSD) decomposition into bias, variance, and phase between simulations and observations for assimilating NEE observations and optimizing all phenology, photosynthesis and post C uptake parameters (P1). Different rows separate the sites as sink (a-c), pivot (d-f) and source (g-i) based on total annual C flux. The sink sites are: US-Vcm, US-Vcp, US-Mpj, US-Fuf, US-Wjs and US-Ses; the pivot sites are: US-Wkg, US-SRG, US-Seg, US-SRM and US-Whs; and the source site ia: US-Aud. The x axes display the optimization scenarios (Prior and P1). The box whiskers show the spread of bias, variance and phase for all 12 sites considered in this study. The bias, variance and phase indicate the mean difference in flux magnitude, the mismatch in terms of flux fluctuation magnitude scales with the mean seasonal amplitude, and the seasonality in flux time series, respectively. Note that the y axis limits are different for all fluxes and site types.

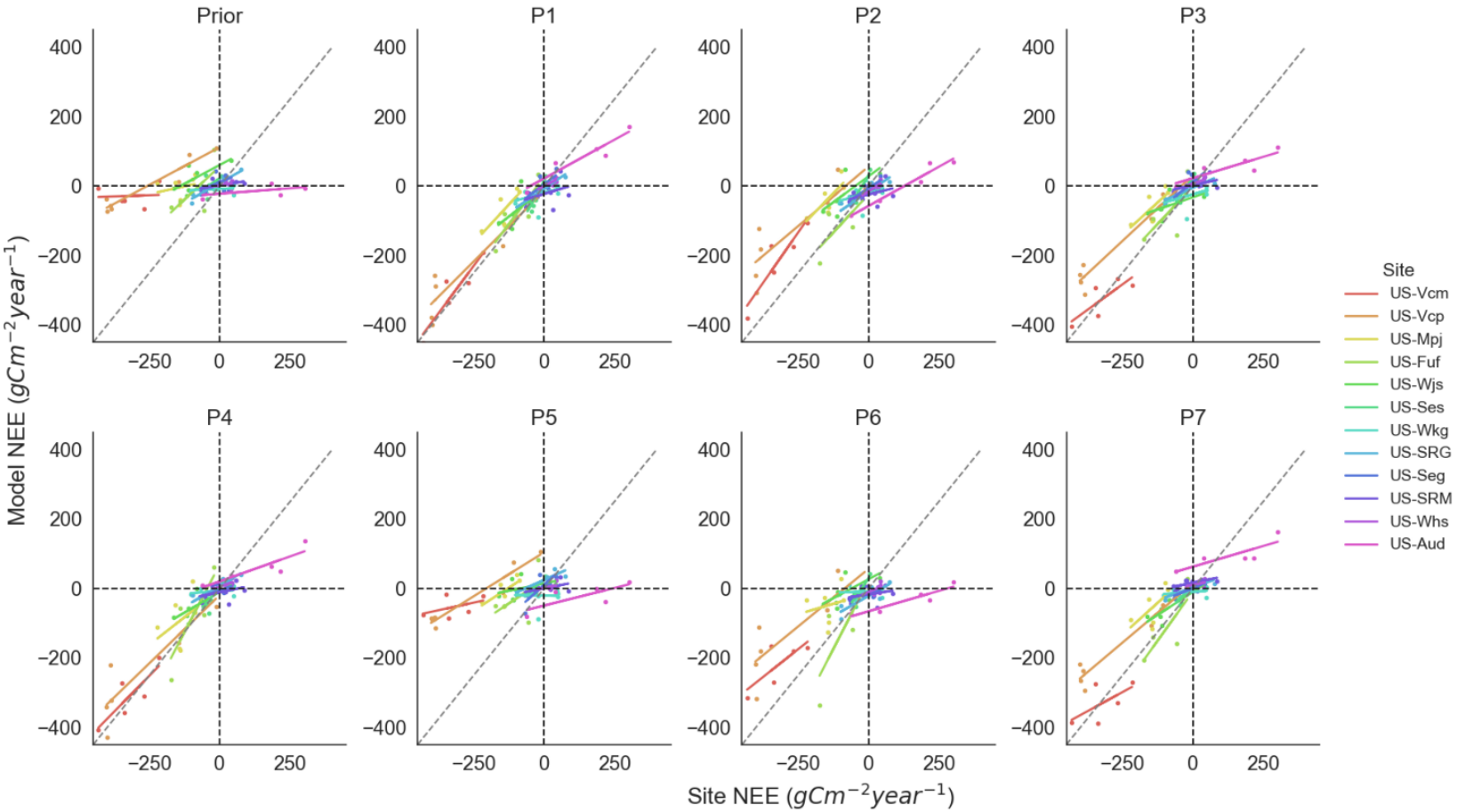

Figure S6. Annual NEE scatter plots for prior and all posterior simulations for assimilating NEE observations with various parameter sets (P1-P7). Different colour legends represent various sites, ordered from the largest mean sink (US-Vcm) to the largest mean source (US-Aud). The middle of the trend line should sit on the 1:1 line if the accurate mean annual source/sink behavior for a site is well captured by the model. A slope value close to or equal to 1 demonstrates the model is better at capturing the IAV. The sink sites are: US-Vcm, US-Vcp, US-Mpj, US-Fuf, US-Wjs and US-Ses; the pivot sites are: US-Wkg, US-SRG, US-Seg, US-SRM and US-Whs; and the source site is: US-Aud.

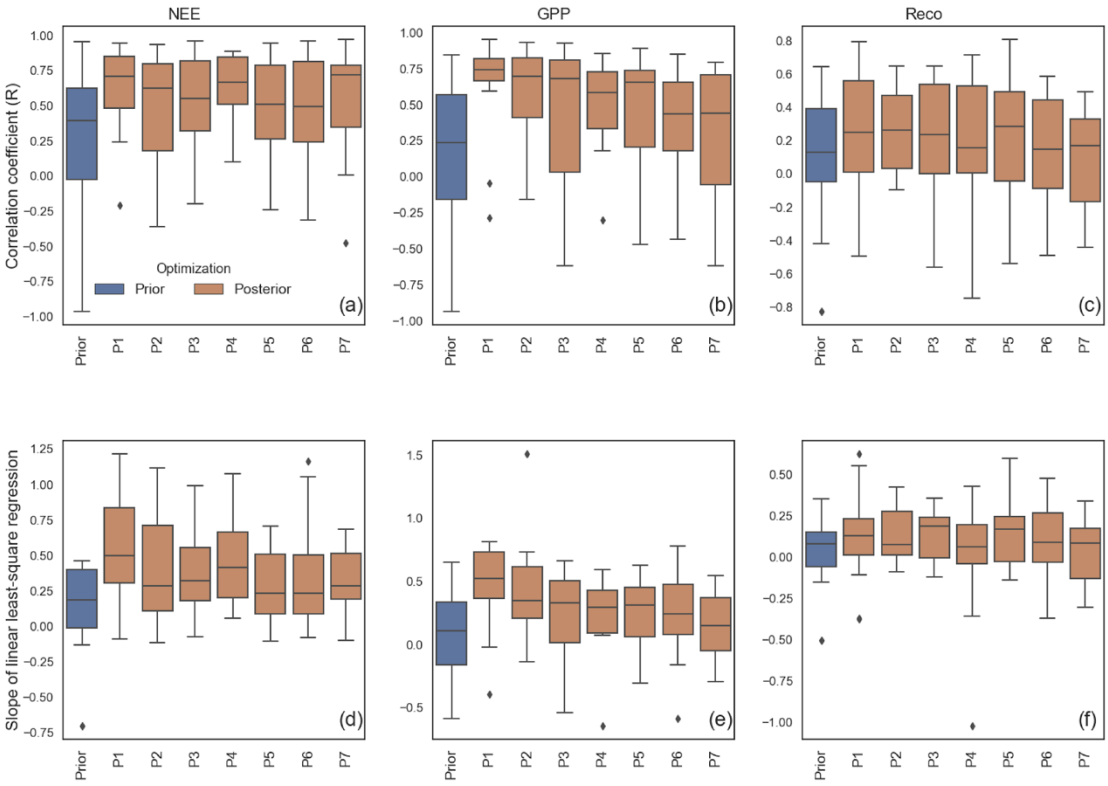

Figure S7. NEE (a, d), GPP (b, e) and R_{eco} (c, f) annual anomaly prior and posterior Pearson correlation coefficients (R) and slope values for the linear regression between model and observed fluxes across all assimilation scenarios with different parameter combinations (P1-P7). The legend represents various assimilation scenarios (Prior - blue bars, and posterior P1-P7 - orange bars).

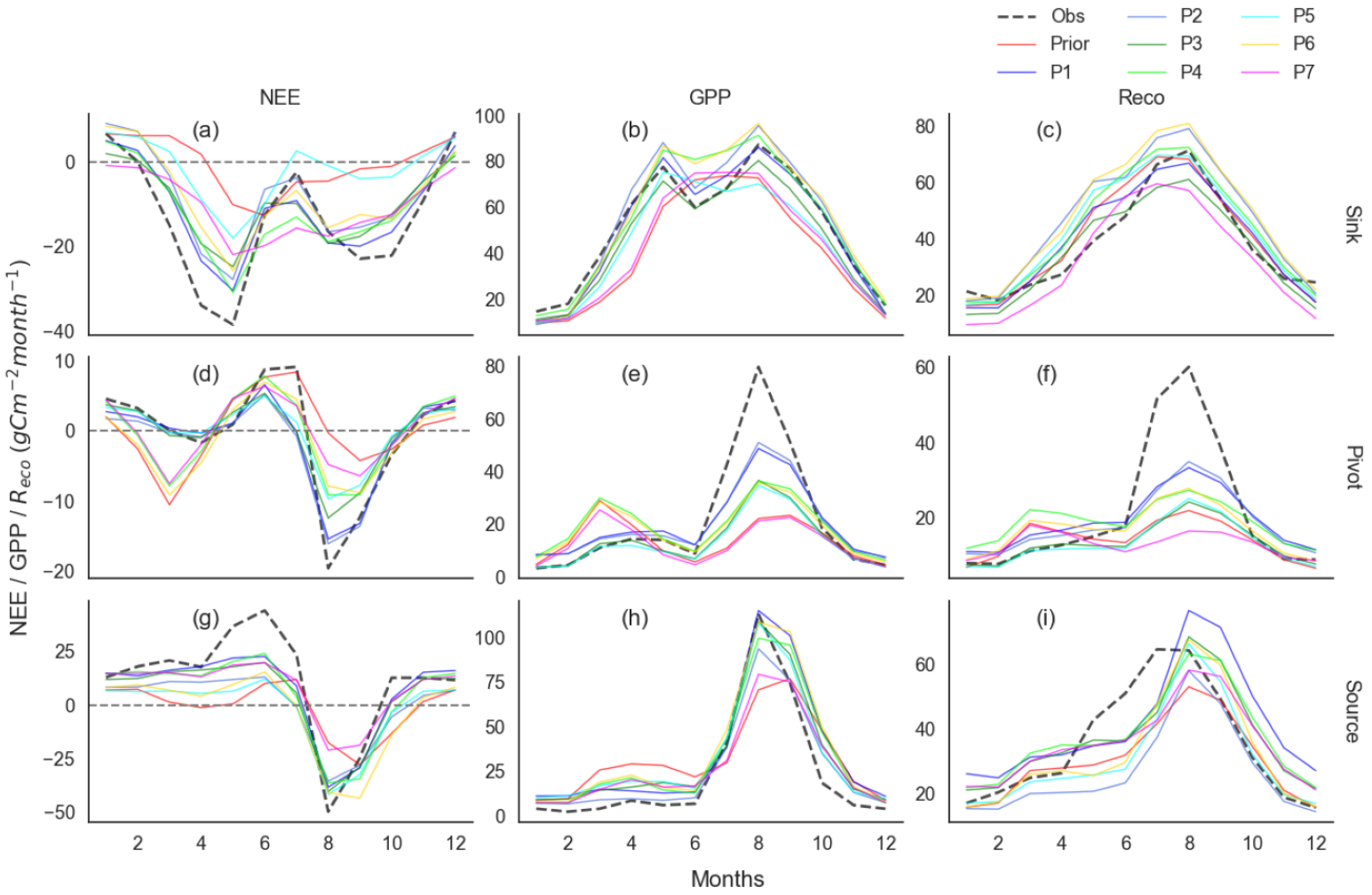

Figure S8. Mean monthly seasonal cycles comparing observations (thick black dashed curve), prior (red curve), and posterior simulations for assimilation scenarios (P1 to P7 – blue to magenta curves) for NEE (left column), GPP (middle column), and R_{eco} (right column) averaged across site C balance types (sink – top row; pivot – middle row; and the source site, US-Aud, on the bottom row).

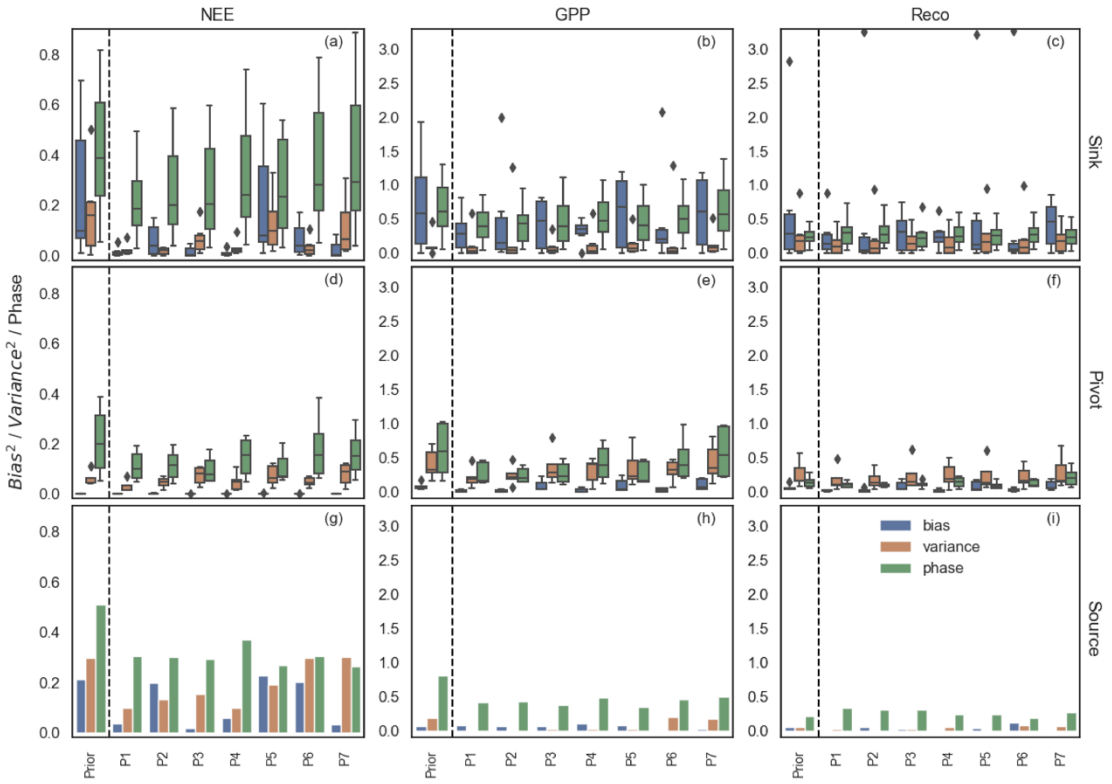

Figure S9. Daily NEE, GPP and R_{eco} mean square deviation (MSD) decomposition into bias, variance, and phase between simulations and observations for assimilating NEE observations with various parameter sets (P1-P7). Different rows separate the sites as sink (a-c), pivot (d-f) and source (g-i) based on total annual C flux. The sink sites are: US-Vcm, US-Vcp, US-Mpj, US-Fuf, US-Wjs and US-Ses; the pivot sites are: US-Wkg, US-SRG, US-Seg, US-SRM and US-Whs; and the only source site is: US-Aud. The x axes display various optimization scenarios (Prior, P1-P7). The parameters included in each optimization are: P1: all parameters; P2: phenology and photosynthesis; P3: phenology and post C uptake; P4: photosynthesis and post C uptake; P5: phenology; P6: photosynthesis and P7: post C uptake. The box whiskers show the spread of bias, variance and phase for all 12 sites considered in this study. The bias, variance and phase indicate the mean difference in flux magnitude, the mismatch in terms of flux fluctuation magnitude scales with the mean seasonal amplitude, and the seasonality in flux time series, respectively. Note that the y axis limits for both gross fluxes are the same.

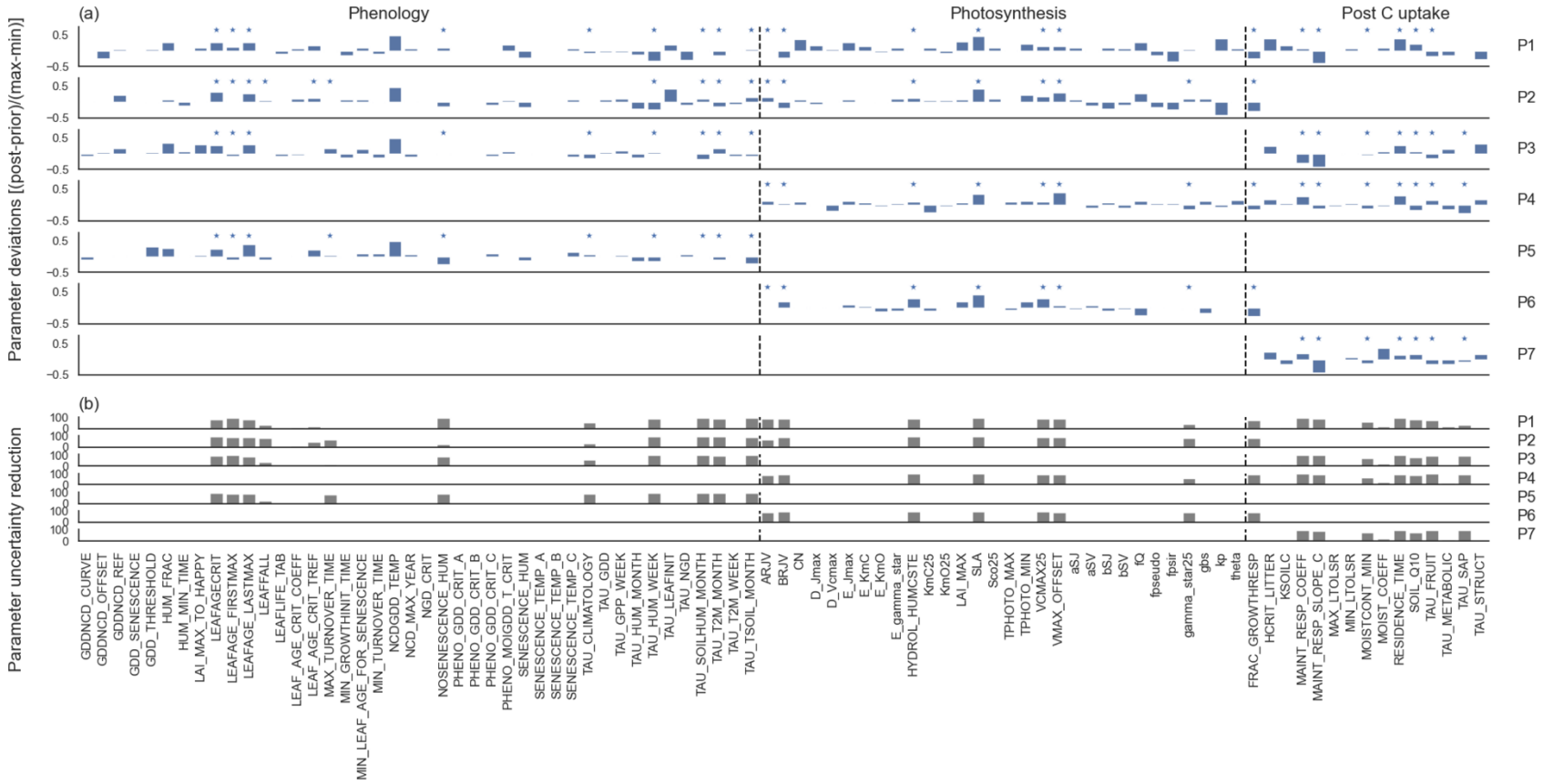

Figure S10. Optimized median parameter deviations [(posterior - prior) / (max - min)] (blue bars) and associated median parameter uncertainty reductions (grey bars) for all parameters controlling phenology, photosynthesis and post C uptake assimilating NEE data (P1-P7). Bars represent the median across all 12 sites. The asterisks above blue bars indicate the parameters that have larger than 50% uncertainty reduction. Each line corresponds to a specific optimization test (shown on the right axis). The parameters are given on the bottom axis. The vertical dashed lines separate the different parameter subsets (phenology, photosynthesis and post C uptake.

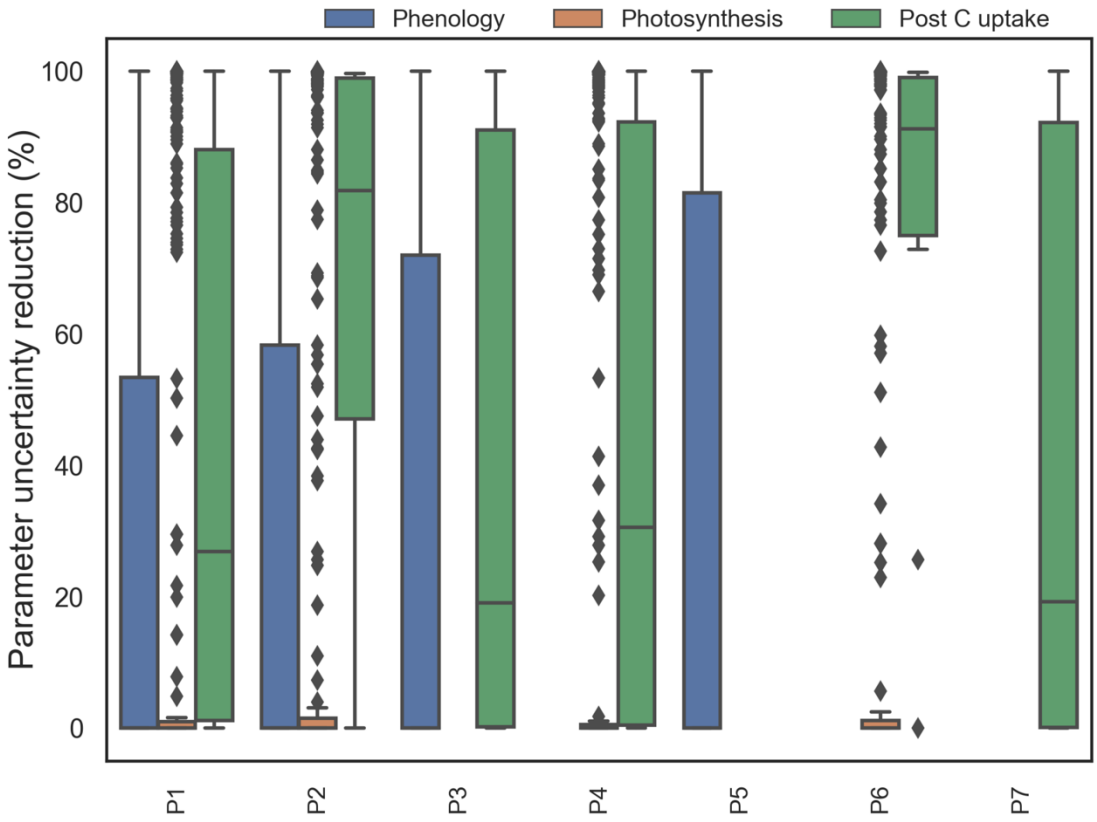

Figure S11. Uncertainty reductions of posterior parameters related to phenology, photosynthesis, and post C uptake across all assimilation scenarios (P1 – P7) shown in x axis.

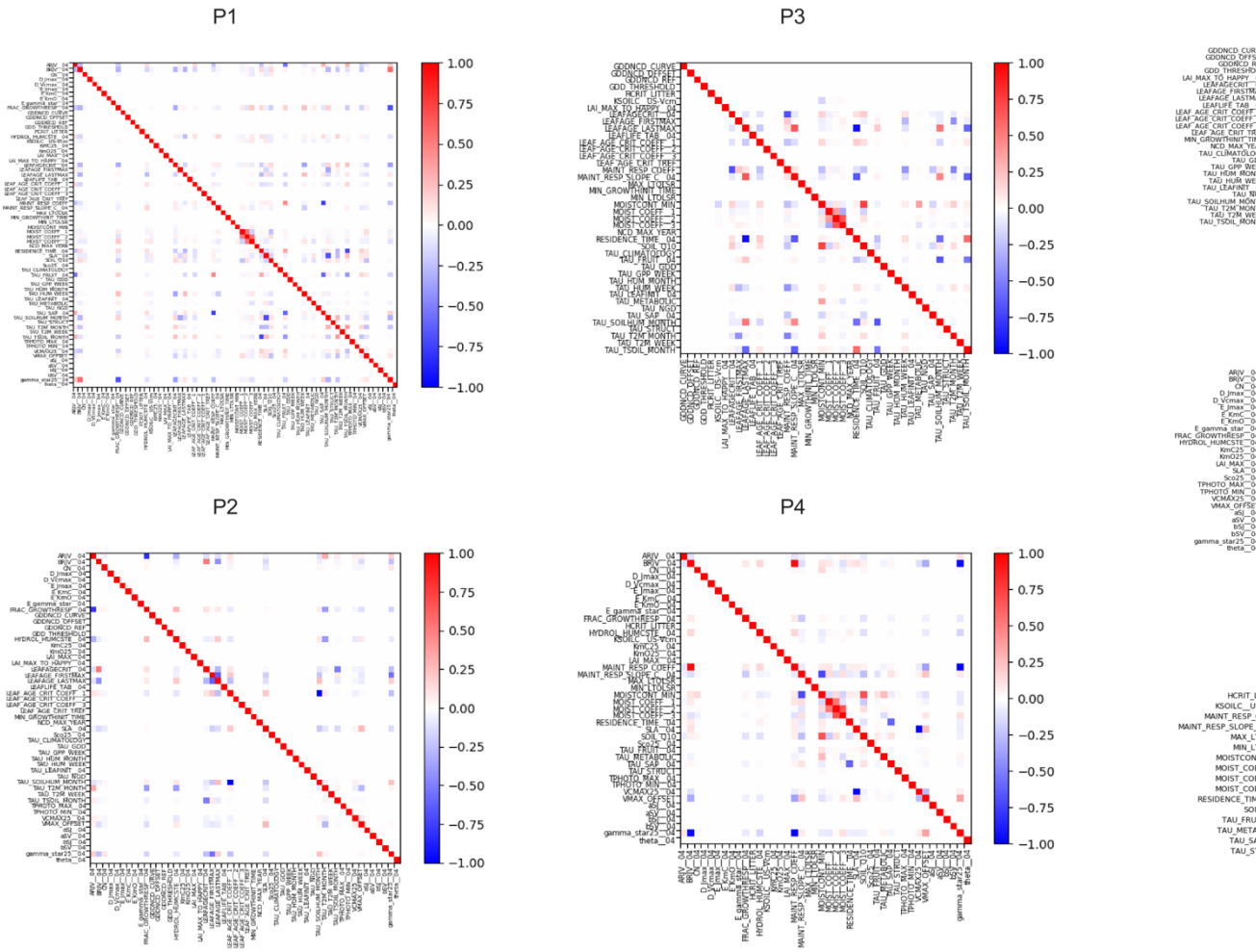

Figure S12. Parameter posterior error covariance matrix for US-Vcm for various assimilation scenarios (P1-P7).

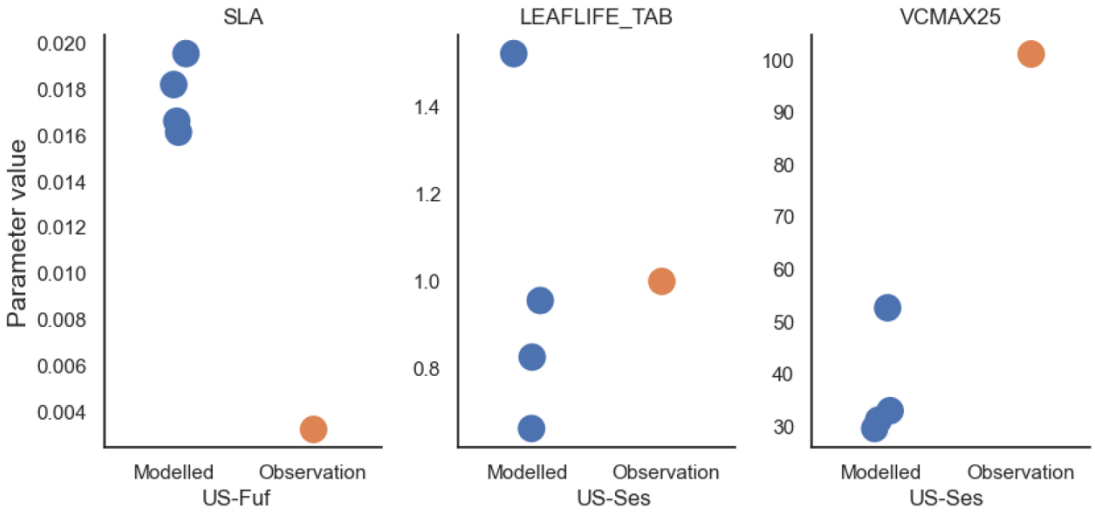

Figure S13. Comparison of posterior parameters against the available trait data from the TRY database. Three comparable traits data are available within 0.5° of the latitude and longitude of each site. These are i) SLA (specific leaf area, unit: m^2/g) for *pinus ponderosa* close to US-Fuf, ii) $V_{c,max}$ (Maximum rate of Rubisco activity-limited carboxylation at 25°C, unit: $\mu mol/m^2/s$) and iii) leaf longevity (LEAFLIFE_TAB, unit: years) for *larrea tridentata* (creosote shrubs) close to US-Ses. Note that all three posterior parameters have values (blue dots) from four assimilation scenarios (both SLA and VCMAX25 are photosynthesis parameters and are included only in P1, P2, P4 and P6 (**Tables 2, S1**); LEAFLIFE_TAB is a phenology parameter and is included only in P1, P2, P3 and P5 (**Tables 2, S1**).

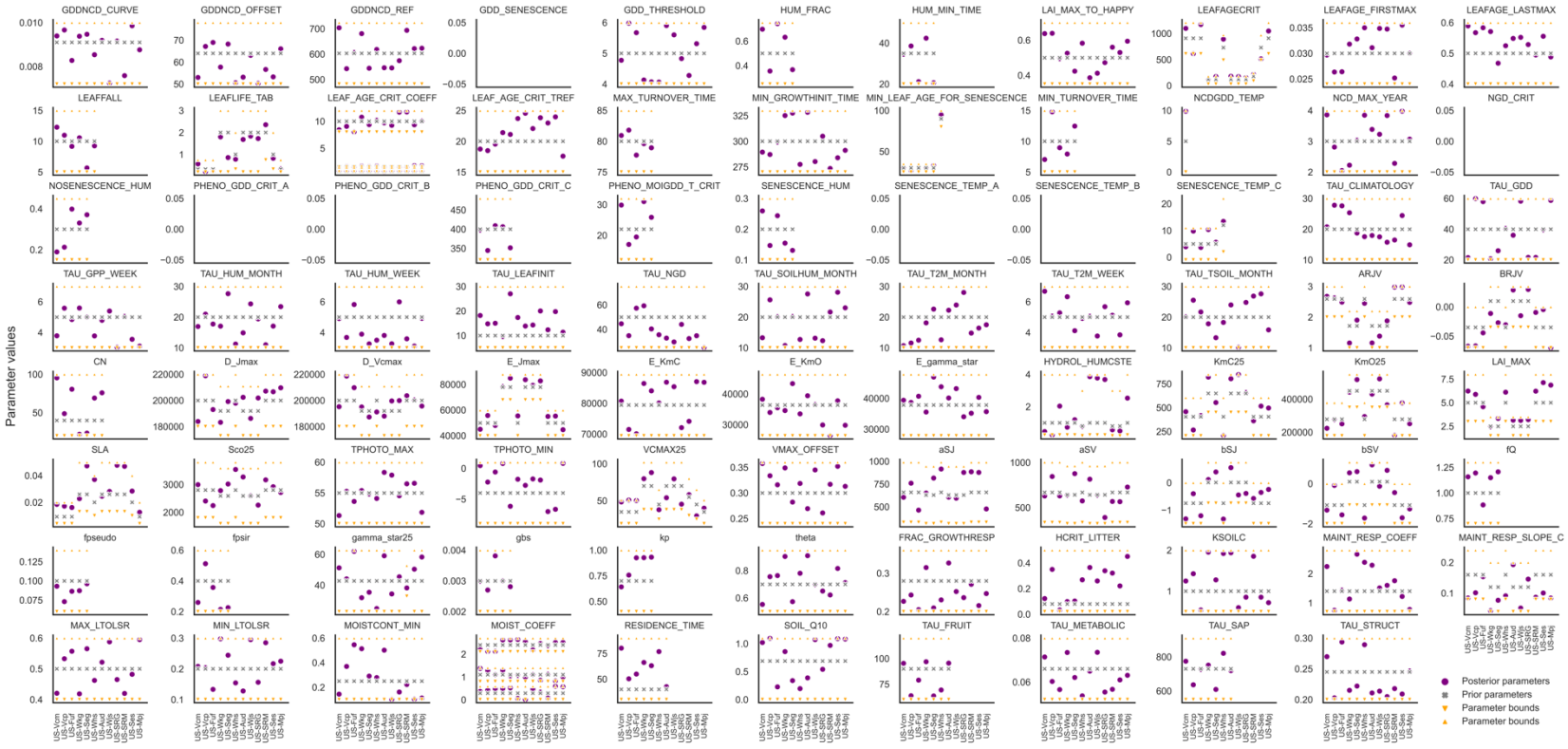

Figure S14. Values of all optimized parameters related to phenology, photosynthesis and post C uptake when assimilating NEE and optimizing all parameters (P1) for all 12 sites. For each parameter, the range of variation (corresponding to yellow arrows), the prior and the posterior values are provided for all sites. For the mixed-PFT sites, only the parameters for the majority PFT fraction are presented, although the other PFT parameters are also optimized. For example, this figure shows the parameters associated with PFT=4 (TeNE) for site US-Mpj, however the optimization is performed with all the parameters of both PFT=4 (TeNE) and 11 (C4G). Note that the soil Q10 parameter is the exponent of the actual Q10 value used to calculate heterotrophic respiration temperature sensitivity (see **Table S1** for more information).

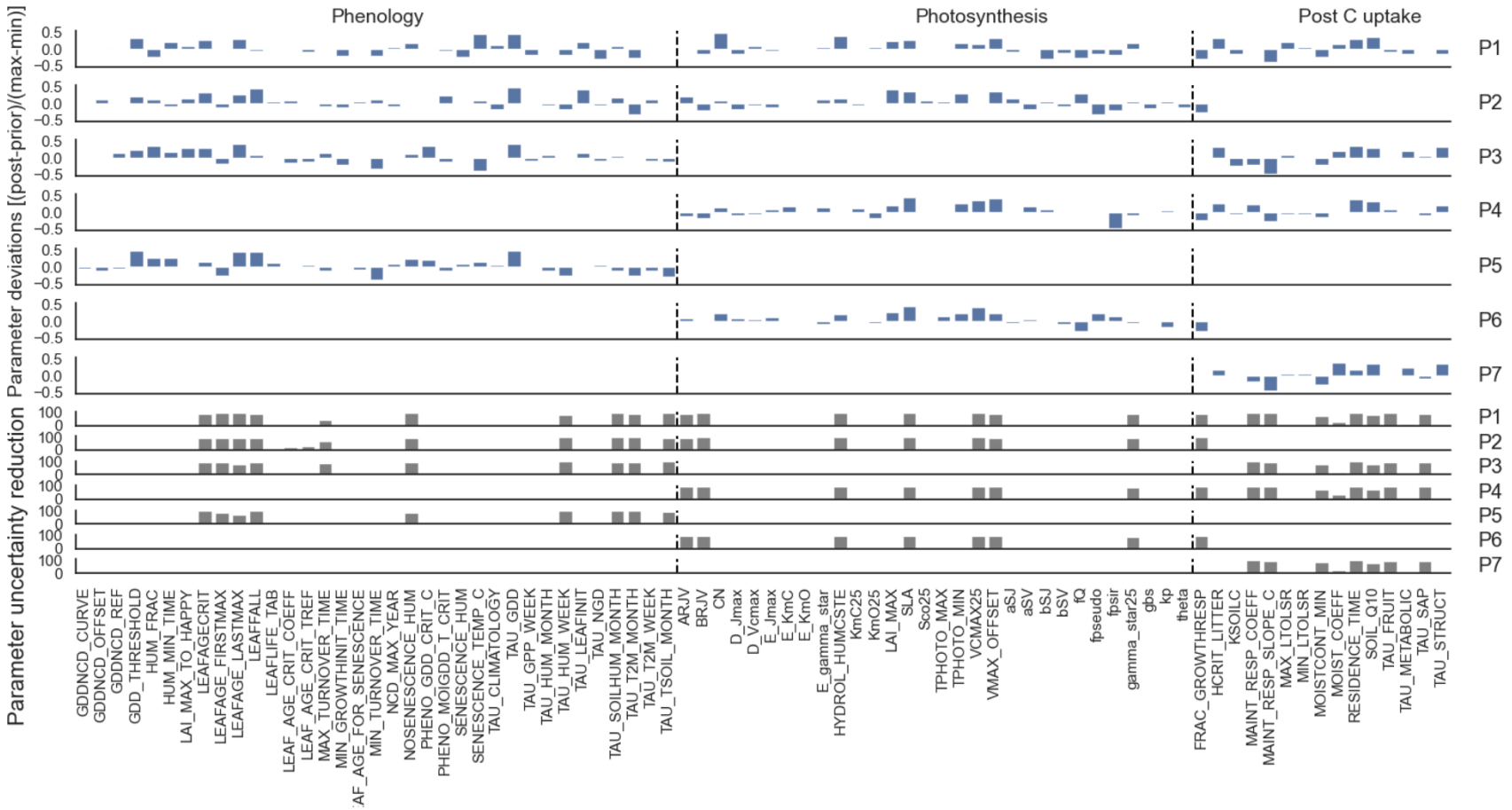

Figure S15. Optimized median parameter deviations [(posterior - prior) / (max - min)] (blue bars) and associated median parameter uncertainty reductions (grey bars) for all parameters controlling phenology, photosynthesis and post C uptake assimilating NEE data (P1-P7). Bars represent the median across all ***sink*** sites.

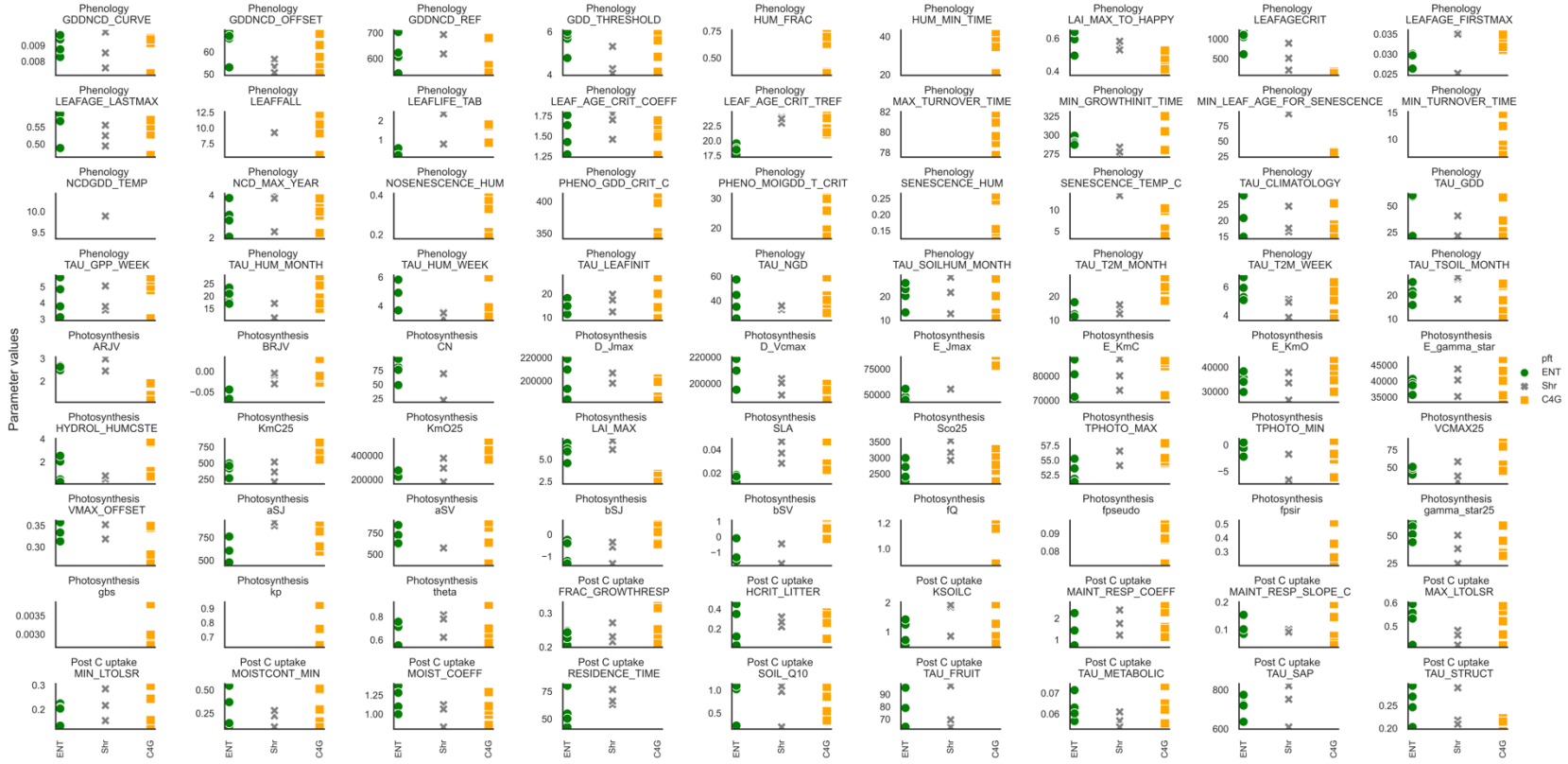

Figure S16. Posterior parameters across 12 sites for each of the main PFTs at each site. Only the parameters with magnitude of deviation > 0.15 and uncertainty reduction of > 50% are listed here with their associated groups (phenology, photosynthesis, and post C uptake). The PFTs are shown in x axes: evergreen needleleaf trees (ENT), shrubs (Shr), and C4 grasses (C4G).